CONCEPTUAL DESIGN STUDY OF THE HIGH LUMINOSITY LHC RECOMBINATION DIPOLE*

G. Sabbi†, X. Wang, LBNL, Berkeley, CA 94720, USA
G. Arduini, M. Giovannozzi, E. Todesco, CERN, Geneva, Switzerland

Abstract

The interaction region design of the High Luminosity LHC requires replacing the the recombination dipole magnets (D2) with new ones. The preliminary specifications include an aperture of 105 mm, with 186 mm separation between the twin-aperture axes, and an operating field in the range of 3.5 T to 4.5 T. The main design challenge is to decouple the magnetic field in the two apertures and ensure good field quality. In this paper, we present a new approach to address these issues, and provide expected harmonics for geometric, saturation and persistent-current effects. The feasibility of an operating field at the high end of the range considered is also discussed, to minimize the D2 magnetic length and facilitate the space allocation for other components.

INTRODUCTION

The HL-LHC recombination dipoles need to generate an integrated force of 35 T·m to direct the incoming beams toward the collision points, and restore parallel trajectories for the outgoing beams. In LHC, this task is performed by a 9.5-m-long two-in-one superconducting magnet with 80 mm coil aperture [1,2]. In order to deflect the beams in opposite directions, the field orientation in the two apertures needs to be the same. This makes the design more challenging than other two-in-one dipoles, since the magnetic flux has to be returned entirely through the iron yoke. In addition, due to the larger beam size in HL-LHC, the coil aperture needs to be increased to 105 mm [3,4]. Including the radial space for cable and collar, the distance between collared coils is reduced to a few cm. In these conditions, the approach adopted for the present D2 magnets, using the iron yoke to decouple the two apertures, leads to large saturation effects [4,5]. We propose an alternative approach where the iron yoke is designed primarily for low saturation, and the resulting large, but current-independent cross-talk between the apertures is corrected with an asymmetric layout of the conductor blocks. This coil design concept is similar to the one adopted for combined function magnets [6], but in this case it is used to compensate, rather than introduce, the higher order multipolar components. The coil cross-section is based on the LHC dipole outer layer cable. The magnetic field calculation was performed using Roxie [7, 8].

* Work supported by the U.S. DOE LHC Accelerator Research Program. The HiLumi LHC Design Study is partly funded by the European Commission within the Framework Programme 7 Capacities Specific Programme, Grant Agreement 284404.
† GLSabbi@lbl.gov

MAGNET DESIGN

Initial Layout and Field Error Definition

A simplified iron yoke design is used to assess the potential of the proposed approach. It has a circular outer diameter (OD) of 560 mm and a central window frame. Full symmetry of the coil and yoke is preserved for the overall twin-aperture magnet with respect to both the horizontal and vertical centrelines (Fig. 1).

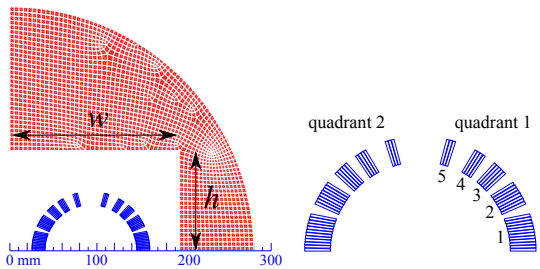

Figure 1: Left: the iron yoke with the central window frame characterized by its half width (w) and half height (h). Right: initial 5-block coil layout (right aperture, top).

The main field and field errors in both apertures are identical except for the opposite signs for the even-order normal harmonics. Thus, the magnetic field quality will be referred only to the right aperture. The magnetic field can be expressed as a series expansion

$$B_y + iB_x = \sum_{n=1}^{\infty} (B_n + iA_n) \left(\frac{x + iy}{R_{\text{ref}}} \right)^{n-1},$$

where B_n is the normal and A_n is the skew multipole coefficients in Tesla at the reference radius R_{ref} [9]. For an aperture of 105 mm, R_{ref} is set to 35 mm. The normal and skew harmonic of order n normalized to the main field in units at R_{ref} are obtained according to $b_n + ia_n = (B_n + iA_n)/B_1 \times 10^4$.

A 5-block layout (Fig. 1 and Table 1) with a frame size of $w = 195$ mm and $h = 115$ mm was selected following a parametric study [10]. In terms of saturation, this layout gives 25 units for b_2 and 20 units for b_3, which are close to the field error target [11].

Asymmetric Coil Layout

The window-frame iron design limits the saturation effect but leads to large cross-talk between apertures (about 200 units of b_2, b_3 for the symmetric coil layout in Fig. 1). To control these errors, we first remove individual turns from conductor blocks based on their contribution to various harmonics. This operation leads to an asymmetric coil layout

Table 1: Coil block parameters for the initial 5-block design (one quadrant). φ and α are the positioning and inclination angles, respectively, expressed in degrees.

Block	No. of turns	φ	α
1	12	0.546	0
2	8	24.5	24.5
3	5	42.5	42.5
4	4	55.7	55.7
5	3	72.2	72.2

within each aperture and turn transitions between blocks at both lead and return ends of the coil. For simplicity of coil winding and end part fabrication, we have limited these asymmetries to a maximum of one turn per block. Figure 2 gives the turn by turn contributions to b_2. With this approach, the harmonics are reduced by about one order of magnitude (b_2 = 29 units, b_3 = −16 units for a main field of 3.5 T).

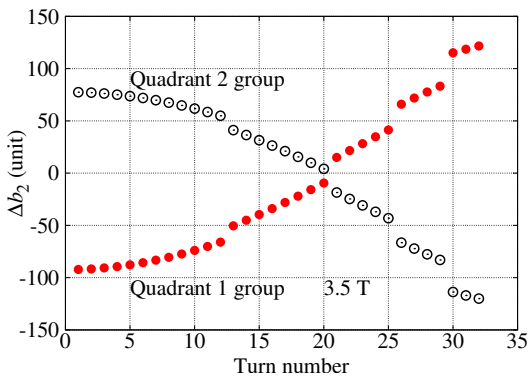

Figure 2: Change in b_2 in the right aperture when one turn is symmetrically removed from the initial layout (Fig. 1). Red points: turns in quadrant 1 of the right aperture (and associated turns for symmetry). Black points: turns in quadrant 2 of the right aperture (and associated turns for symmetry).

Coil Block Displacement

After a few redistributions of turns among blocks to reduce the low-order harmonics, it becomes more effective to further reduce the field errors by adjusting the positioning angles φ and α as shown in Table 2 and Fig. 3.

Table 2: Sensitivity (unit/degree) of the harmonics to the two modes of φ change as shown in Fig. 3.

	b_2	b_3	b_4	b_5	b_6	b_7	b_8	b_9	b_{10}
φ_1	-2	-38	0	-32	0	-17	0	-7	0
φ_2	-50	-1	-31	0	3	0	9	0	3

At this stage, one additional iteration on the window frame parameters is performed (h = 120 mm and w = 195 mm) to further reduce the harmonics and saturation.

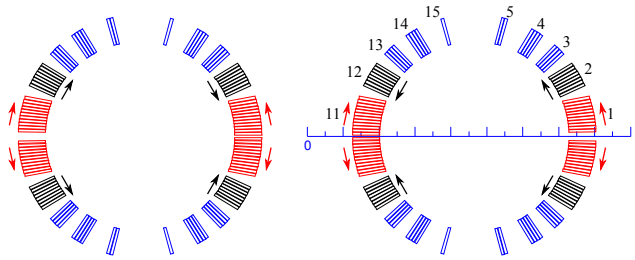

Figure 3: Two modes of positioning angle change. The arrows indicate displacement direction (away from midplane for positive φ). 1) Red blocks to tune the odd-order harmonics (dipole symmetry). 2) Black blocks to tune the even-order harmonics (no dipole symmetry, but symmetric with respect to x = 0).

Numerical Optimization

The previous steps bring the harmonics to sufficiently low values to allow effective automatic optimization using Roxie. The Extrem algorithm option is used to minimize the weighted sum of the harmonics at 3.5 T with a focus on low-order terms. Since the field errors are more sensitive to φ than to α, we vary φ for each coil block in the first and second quadrants in the right aperture. The parameters for the optimized coil blocks are given in Table 3.

Table 3: Coil block parameters for the Roxie-optimized cross section (block numbers are given in Fig. 3, φ and α are expressed in degrees).

Block	No. of turns	φ	α
1	11	2.1207	0.9
2	8	25.49	24.5
3	4	44.224	42.5
4	4	57.444	55.7
5	2	76.74	73.97
11	12	0.5584	0
12	8	24.062	24.5
13	4	42.621	42.5
14	4	58.017	55.7
15	1	80.491	73.97

EXPECTED FIELD QUALITY

The expected field quality is computed considering the geometric, saturation and persistent-current effects at 1.9 K. The main field transfer function has a geometric component of 0.368 T/kA. Saturation starts to be significant at about 2900 A. The transfer function reduces by 8.9% at 3.5 T. The corresponding current is 10.5 kA and the peak field in the coil is 4.1 T.

Figure 4 shows the computed b_2. For field errors, the geometric component is defined at 100 A (0.04 T) along the black line in Fig. 4. Saturation is given by the difference between the harmonics at 100 A and nominal current. The persistent-current contribution is the difference between the

ISBN 978-3-95450-132-8

harmonics at the injection level (0.25 T, 675 A) and the geometric values.

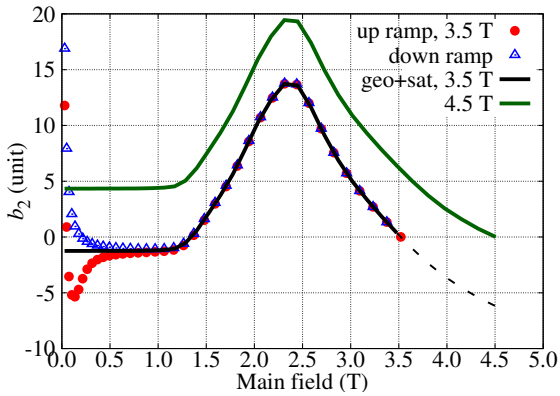

Figure 4: The calculated b_2: geometric and saturation effects for the coil optimized at 3.5 T (black line) and at 4.5 T (green line); persistent-current effect for the 3.5 T layout at 1.9 K (red dots, blue triangles).

Table 4 summarizes the expected field errors. The skew harmonics are zero due to the top-bottom coil symmetry. Lower-order geometric errors generally meet the targets [11]. The geometric errors for harmonic order $n > 9$ are in the range of 0.5 to 1.5 units, which is larger than the initial targets. They should be evaluated and if required, further reduced with additional cross-section optimization. The saturation effects for the low-order terms are all lower than the targets. The effect does not vary monotonically with current for harmonic order $n < 5$. The impact of this behaviour on beam dynamics should be investigated.

Table 4: Expected field errors (in units at $R_{\text{ref}} = 35$ mm). The saturation quoted in parenthesis indicates the peak value due to the non-monotonic behaviour (Fig. 4).

n	Geo.	Sat.	Pers.	Inj.	3.5 T
2	-1.25	1.25 (14)	-1.91	-3.15	0.01
3	1.77	-1.76 (7)	-14.68	-12.91	-0.48
4	1.96	-1.92 (3)	1.23	3.19	0.09
5	0.94	-1.01	1.20	2.15	-0.15
6	0.34	-0.37	-0.21	0.13	-0.02
7	0.19	-0.09	-0.01	0.19	0.07
8	0.18	-0.01	0.11	0.29	0.18
9	-0.42	-0.05	0.04	-0.38	-0.48
10	-0.25	-0.03	-0.17	-0.42	-0.27
11	1.28	0.13	0.15	1.43	1.41
12	-1.38	-0.13	-0.01	-1.38	-1.51
13	0.54	0.05	-0.08	0.45	0.59
14	0.09	0.01	-0.02	0.07	0.10
15	-1.45	-0.14	-0.07	-1.52	-1.59

At injection level, the quadrupole (b_2) error is dominated by the persistent-current effect. The sextupole (b_3) is larger than the target value due to a reduced compensation effect with respect to its geometric value. At 3.5 T, the low-order harmonics are close to the target values. The high-order terms are dominated by the geometric components.

FEASIBILITY OF OPERATION AT 4.5 T

Increasing the main field from 3.5 T to 4.5 T reduces the magnetic length from 10 m to 7.8 m and facilitates the space allocation for other components. By repeating the optimization process at 4.5 T, the harmonic content is similar to the one previously obtained at 3.5 T (Table 4). At the nominal current of 13850 A, the peak/bore field ratio is 1.18. As shown in Fig. 5, the 4.5 T operation point is at 70% of the load line, up from 54% for the 3.5 T layout, but still within the initial design target.

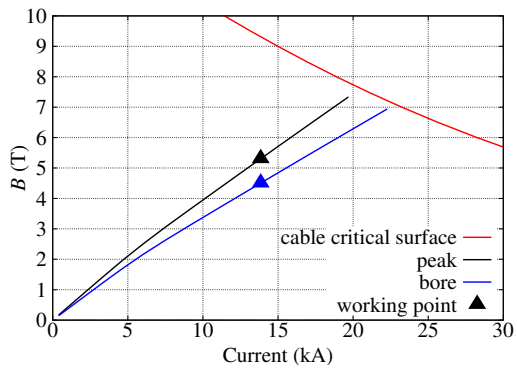

Figure 5: Load line for the coil layout optimized at 4.5 T. The maximum load line working point is 70%.

Assuming that a cryostat with a shell thickness of 10 mm is positioned concentric with the magnet, the fringe field at a radius of 501 mm ranges from 45 to 105 mT at 4.5 T. The fringe field can be reduced by increasing the yoke diameter from the 560 mm assumed for this study. In addition, a more detailed yoke optimization beyond the simple window-frame considered for this study is expected to yield improved performance in terms of operating margin, saturation effects and fringe field.

SUMMARY

The LHC recombination dipole magnets will need to be upgraded to a larger aperture for the High-Luminosity LHC project. The main design challenge is to decouple the magnetic field in the two apertures and to ensure good field quality. A magnetic design study based on the LHC dipole cable was performed where the iron yoke is designed primarily for low saturation effects, and the field errors are corrected with an asymmetric coil layout. The estimated field harmonics for geometric, saturation and persistent-current effects are provided and compared to the latest error table (version 1.4, 2013). The feasibility of increasing the operating field from 3.5 T to 4.5 T, with the magnetic length decreasing from 10 m to 7.8 m, was discussed in terms of operating point, field quality and fringe field. Tracking studies to assess the compatibility of the estimated error table with beam dynamics requirements are in progress and preliminary results are reported in Ref. [12].

REFERENCES

[1] O. S. Brüning, P. Collier, P. Lebrun, S. Myers, R. Ostojic, J. Poole, and P. Proudlock, Eds., *LHC Design Report*. Geneva: CERN, 2004, vol. 1, ch. 8, pp. 230–234.

[2] E. Willen, M. Anerella, J. Cozzolino, G. Ganetis, A. Ghosh, R. Gupta, M. Harrison, A. Jain, A. Marone, J. Muratore, S. Plate, J. Schmalzle, P. Wanderer, and K. C. Wu, "Superconducting dipole magnets for the LHC insertion regions", EPAC'00, Vienna, June 2000, pp. 2187–2189, http://www.JACoW.org

[3] R. De Maria, S. Fartoukh, A. Bogomyagkov, and M. Korostelev, "HLLHCV1.0: HL-LHC layout and optics models for 150 mm Nb_3Sn triplets and local crab-cavities", IPAC'13, Shanghai, May 2013, pp. 1358–1360, http://www.JACoW.org

[4] E. Todesco, H. Allain, G. Ambrosio, G. Arduini, F. Cerutti, R. De Maria, L. Esposito, S. Fartoukh, P. Ferracin, H. Felice, R. Gupta, R. Kersevan, N. Mokhov, T. Nakamoto, I. Rakno, J. Rifflet, L. Rossi, G. Sabbi, M. Segreti, F. Toral, Q. Xu, P. Wanderer, and R. van Weelderen, "A first baseline for the magnets in the high luminosity LHC insertion regions", IEEE Trans. Appl. Supercond., vol. 24, no. 3, p. 4003305, June 2014.

[5] R. Gupta, "Conceptual magnetic design of 105 mm aperture dipole D2", https://indico.fnal.gov/conferenceDisplay.py?confId=6164, April 2013, presentation at joint LARP/HiLumi-LHC Collaboration Meeting.

[6] T. Nakamoto, N. Higashi, T. Ogitsu, A. Terashima, Y. Ajima, M. Anerella, R. Gupta, H. Hattori, T. Ichihara, Y. Iwamoto, N. Kimura, Y. Makida, T. Obana, K.-I. Tanaka, P. Wanderer, and A. Yamamoto, "Design of superconducting combined function magnets for the 50 GeV proton beam line for the J-PARC neutrino experiment", IEEE Trans. Appl. Supercond., vol. 14, no. 2, pp. 616–619, June 2004.

[7] S. Russenschuck, "ROXIE – a computer code for the integrated design of accelerator magnets", EPAC'98, Stockholm, June 1998, pp. 2017–2019, http://www.JACoW.org

[8] S. Russenschuck, *Field Computation for Accelerator Magnets: Analytical and Numerical Methods for Electromagnetic Design and Optimization*. (Weinheim: John Wiley & Sons, 2010).

[9] A. K. Jain, "Basic theory of magnets", in *CERN Accelerator School: measurement and alignment of accelerator and detector magnets*, 1998, no. CERN-98-05, pp. 1–26.

[10] G. Sabbi and X. Wang, "Design study of the high luminosity LHC recombination dipole (D2)", Lawrence Berkeley National Laboratory, Tech. Rep. LBNL-6651E, May 2014.

[11] E. Todesco, "D2 field error tentative table", https://lhc-div-mms.web.cern.ch/lhc-div-mms/tests/MAG/docum/hilumi/Magnets/field_quality.xlsx, October 2013, version 1.4.

[12] Y. Nosochkov, Y. Cai, M.-H. Wang, R. De Maria, S. D. Fartoukh, M. Giovannozzi, and E. McIntosh, "Specification of field quality of the interaction region magnets of the high luminosity LHC based on dynamic aperture", IPAC'14, Dresden, Germany, June 2014, TUPRO008, these proceedings.

ISBN 978-3-95450-132-8